Two-dimensional modeling of flooding in Fragoso River floodplain with tidal influence in Olinda city (Brazil)

Arivânia Bandeira Rodrigues (arivania.rodrigues@ufpe.br)

Federal University of Pernambuco: Universidade Federal de Pernambuco https://orcid.org/0000-0003-0452-0006

JAIME CABRAL

University of Pernambuco: Universidade de Pernambuco

Research Article

Keywords: Two-Dimensional Hydrodynamic Modeling, Lidar, Flood Risk, Fragoso River-PE, Brazil

Posted Date: May 26th, 2022

DOI: https://doi.org/10.21203/rs.3.rs-1534551/v1

Abstract

Population growth and consequent changes in land use associated with climate change have proved that traditional drainage methods are inefficient. As a result, the need for new techniques has emerged, such as flood simulations for risk and danger assessment using two-dimensional resolutions of flood wave propagation for flooding problems in urban areas. Thus, the present work sought to evaluate structural measures and their effects on floods in a case study in Olinda city in response to different rainfall events in Fragoso River Basin, Pernambuco State (Brazil). This region has a disordered urbanization process associated with a vulnerable drainage system. Several scenarios were evaluated to obtain the floodable areas and hazard indicator maps, with simulations before and after the construction of the Fragoso channel. PCSWMM and HEC-RAS software were used to perform hydrological and two-dimensional hydrodynamic modeling. For land use characterization, MapBiomas data were applied. Lidar technology project with laser terrain survey (the so-called Pernambuco Tridimensional - PE3D) was used for geomorphology data. Simulation results were satisfactory for a better understanding of the flooding area. Comparing simulations before and after Fragoso channel completion, a reduction in the total flooded area was obtained, but the flooding problems will persist. Results of this study can contribute to informing risk assessments and support decision-making regarding flooding in estuarine plains.

Introduction

The development of modern society, predominantly urban, has occurred in a disorderly way, with high rates of population growth, without any planning, at the expense of increasing levels of pollution and environmental degradation. As a result of this unbalanced scenario, there are significant impacts on urban infrastructure, especially water resources (Braga et al., 2005). With heavy rains, floods, and the greater concentration of population and goods in urban areas, devastating flood disasters frequently occur worldwide. There are concerns that flood damage will harm local economic development, threaten the sustainability of local communities, and negatively affect supply chains and, therefore, global economic activities (Itagaki et al. 2021).

The last few decades have seen a growing interest in the study of floods, their consequences on society and natural ecosystems, and the development of measures to reduce their impact. Flood risk maps are among the most important tools for managing flood risk. As defined by the European Floods Directive (European Commission, 2007), flood risk maps are designed to indicate the probability and magnitude of different flood scenarios in a given area. They are used as decision-making tools for various purposes, from infrastructure planning and development to disaster response (Nogherotto et al. 2021).

The occupation of irregular areas puts the population at a practical risk situation, making it vulnerable to disaster situations and contributing to the degradation of the environment. The problem of flooding is increasingly present in urban centers and has a considerable impact on the security and stability of the community. The disorderly growth of cities directly affects land use, with its consequent impermeabilization, increasing the volume of water drained. This unplanned growth, combined with

increasingly less predictable climate change, has worsened the world scenario of disasters caused by floods (Tucci 2004).

Hodgkins et al. (2019) analyzed data from 1465 watersheds in the United States from 1941 to 2015. They found that most watersheds that received flow regularization works had their annual flow peaks reduced, while most urbanized watersheds tended to increase the annual flow peaks.

According to the sixth assessment report of the Intergovernmental Panel on Climate Changes (IPCC), in a world scenario, climate risks based on extreme rainfall and coastal flooding are already moderate to high, with a high confidence index in the uncertainty of forecasts. Therefore, we are warning that during the next two decades, human societies will face a series of inevitable climatic risks caused by global warming that moves in the direction of 1.5ºC, which is currently 1.1ºC over the industrial period (IPCC, 2021). Furthermore, a recent study using revised coastal elevation data found that the number of people threatened by projected sea-level rise and coastal flooding in 2100 could be three times higher than previous estimates (Kulp and Strauss 2019).

The probability of coastal flooding has been increasing globally since this portion of the population is more vulnerable to the possible impacts of climate change. By the year 2050, economic losses in the order of US$ 940 million are estimated in average annual losses if the sea level rises by 20 cm in the 22 largest coastal cities in Latin America and the Caribbean, exceedingly more than US$ 1 billion in the case 40 cm rise from sea level (Adams et al., 2014). Natural disasters caused by floods are among the most damaging events in terms of social and economic losses, both in European countries as well as in China, the United States, Myanmar, the Philippines, Pakistan, Iran, Saudi Arabia, Egypt, and Venezuela, which were affected and suffered floods (Elkhrachy et al. 2021).

In this context, the city of Olinda has geographic and urban peculiarities that make it highly susceptible to flooding. The low elevations of its territory about sea level, high rainfall, low hydraulic gradient, high water table, tidal influence, and the high rate of soil impermeabilization contribute to recurrent flooding.

The mapping of areas susceptible to flooding is a fundamental element for defining non-structural measures in the search for the development of flood risk management strategies, including spatial planning, land use, and occupation and civil defense plans. Furthermore, this mapping can be developed using different methodologies and support instruments and subsidize the reorganization of urban space since they can be helpful in the establishment of new occupation guidelines in a city (Frank, Pinheiro 2003 and Momo et al. 2016).

For this, the study was based on the results through hydrological modeling, using mathematical models capable of reproducing the hydrological cycle and thus mirroring the surface runoff as a consequence of the rainy event, using the SWMM model (Storm Water Management Model) developed by the United States Environmental Protection Agency (US EPA). In addition, the hydrodynamic simulation is also relevant because it can reproduce the behavior of the flow propagation along the water body using the

HEC-RAS 5.0.7 model (Hydrologic Engineering Center – River Analysis System) developed by the Army Corps of Engineers. The United States "US Army Corps of Engineers".

The present work applies hydrological and hydrodynamic modeling of the Fragoso River basin in Olinda, which occupies a very low-level plain in its low stretch, suffering the effect of the tides and presenting many flooding problems. Simulations of different rainfall scenarios were carried out, and situations of project execution were analyzed as subsidies for the management of rainwater in the municipality.

Methodology

2.1 Study area

The watershed of the Fragoso River is located in the Metropolitan Mesoregion of Recife, in the Water Planning Unit UP-14, GL1 of the group of small coastal rivers, on the northern coast of the State of Pernambuco, Brazil. It is mainly located in the municipality of Olinda, with an occupation of 62%, and a minor part, in the cities of Paulista and Recife, with an occupation of 35% and 3%, respectively. The Fragoso River has a length of about 14.7 km, from its source to its mouth in an estuary together with the Paratibe River. The Fragoso river basin has a contribution area of 28.6 km² and an estimated 268 thousand inhabitants. The main tributaries are Ouro Preto and Bultrins streams, as shown01. The Fragoso river in the plain stretch is undergoing a significant intervention with widening and deepening of the gutter as well as concreting the bottom and sides. This section of the interventions is being called Fragoso Chanell.

2.2 Hydrological Modeling

For the delimitation process of the Fragoso river basin and later of the sub-basins, data from the Pernambuco Tridimensional (PE3D) program were used, which carried out laser scanning and obtained high-resolution orthoimages of the entire territorial surface of Pernambuco, obtaining the model Digital Terrain (MDT), with altimetric accuracy better than 25 cm with a scale of 1:5,000. The technology used to obtain the images is LiDAR (Light Detection and Ranging), with data capture performed by sensors and cameras installed in airplanes (Cirilo et al. 2014). High-resolution data provide more accurate local topography and friction estimates and help reduce flood modeling uncertainty (Brussee et al. 2021).

The SWMM program – Storm Water Management Model – is a widespread hydrological-hydraulic model developed by the U.S. EPA (the United States Environmental Protection Agency), in constant use, mainly used for simulations in urban areas to assist in the planning, analysis, and design of stormwater drainage projects. It consists of a rainfall-runoff model that continuously simulates surface runoff quantity and quality in punctual and long-term rainfall events (Rossman 2016).

The PCSWMM software has an interface with the GIS environment, thus facilitating the insertion of sub-basins and conduits obtained previously with the delimitation of the basin. Microdrainage was not considered in this analysis due to a lack of data. Instead, junctions/Nodes were inserted, assigning them

topographic dimensions, Conduits indicating the length, Manning coefficient, and section. The following parameters and variables were also added to the sub-basins. For the outlet, the tidal curve was considered.

The parameters necessary for the hydrological simulation of the area under study are the physical characteristics of each contributing sub-basin (area, percentage of permeable and impermeable area, representative width, slope, Manning roughness coefficient, and height of storage in depressions). In addition, other variables such as precipitation, infiltration, and tide were also analyzed and applied to the model.

The hydrological model used hourly data from six rainfall stations operated by Cemaden (National Center for Monitoring and Alert of Natural Disasters) as input data. The simulated event took place on May 30, 2016, lasting 16 hours, starting at 00:00. The impacts resulting from this event were reflected in the suspension of classes at dozens of public and private schools and colleges and working hours in private companies and public bodies. Urban mobility was also compromised, including buses and trucks.

Table 01 presents the rainfall stations used by Cemaden and the location according to geographic coordinates and the total rainfall for each station.

Table 01 – Data from the rainfall stations used in the Fragoso River Basin in Olinda-PE for 16 hours on May 30, 2016. Source: Prepared by the author.

Pluviometric Station	Latitude (UTM)	Longitude (UTM)	The total precipitate (mm)
Jardim Fragoso - Olinda	295723.39 E	9116966.29 S	241.5
Tabajara - Olinda	294063.97 E	9118175.53 S	230.6
Bonssucesso - Olinda	295955.84 E	9114312.68 S	212.9
Aguazinha - Olinda	291982.10 E	9115290.13 S	196.3
Águas Compridas - Olinda	289217.41 E	9117047.20 S	162.3
Janga 2 – Paulista	298244.65 E	9120295.82 S	210.2

To perform simulations with different return times, the intense rain equation developed in the Recife Urban Drainage Master Plan (Equation 1) was used, which has been used by cities in the Metropolitan Region of Recife (Recife 2016).

$$i = \frac{611{,}3425\ x\ T^{0{,}1671}}{(t + 7{,}3069)^{0{,}6348}} \qquad \text{Equation 1}$$

Where: i = precipitation height of duration t (mm); i_1, i_2 = rainfall intensity (mm/h); T = retorn period (years); t = duration of rain in minutes.

Thus, using the rainfall event that occurred on May 30, 2016, as a reference, tide records were obtained from the tide table of the Port of Recife at the Center for Weather Forecasting and Climatic Studies (CPTEC) of the National Research Institute. (INPE), presented in Table 02, and then the tidal curve was performed for the time interval of 1 hour, considering the 16 hours of the simulated event, through the analytical method from the knowledge of water heights (Hydrographic Institute 2018).

Table 02 - Tide data for the Port of Recife on 05/30/2016. Source: CPTEC (2020)

Time	Height (m) Relative to the zero of the tide	Height (m) Brazilian Institute for Geography and Statistics (IBGE)
04:30	0,70	-0,44
10:45	2,00	0,86
17:15	0,60	-0,54
23:24	1,90	0,76

2.3 Hydrodynamic Modeling

The hydrodynamic modeling was performed using HEC-RAS 5.0.7 (Hydrologic Engineering Center - River Analysis System), public domain software developed by the United States Army Corps of Engineers "US Army Corps of Engineers", which aims to perform One-dimensional and two-dimensional hydraulic calculations for natural and artificial river and chanell network (Usace 2016a).

In two-dimensional modeling in a non-steady regime, the model uses the two-dimensional Shallow Water equations (also called two-dimensional Saint-Venant equations, referring to the continuity and momentum equations) or the Diffuse Wave equations. The discretization of the Diffuse Wave equations is performed using the finite difference method for time and a hybrid scheme combining the finite difference and finite volume methods for space discretization (Usace 2016b).

In the model for carrying out the 2D simulations, the Digital Terrain Model (MDT) obtained from the PE-3D data, tidal data interpolated every hour, and the flows for each sub-basin obtained from the PCSWMM hydrological model were used. It was prioritized to carry out the hydrological simulation in the PCSWMM software to analyze better the flow results obtained since, with this software, the surface runoff becomes more sensitive to urbanization. Due to some input data, such as permeable and impermeable areas, as well as be possible to carry out simulations with applications of sustainable urban drainage techniques. The coupling of hydrological and hydrodynamic modeling provides a complete representation of the surface water flow process, which can be applied in several simulations. As a result, some results can be obtained, such as mapping floodable areas and risk and danger indices, evaluating the efficiency of measures structural and compensatory techniques, and assisting in developing a flood warning system.

For the study area, the orthophotos were obtained in February 2016, while the laser-scanned in December 2015. Thus, changes in the terrain between December 2015 and May 2016 were compared with Google Earth images. A period in which the precipitation event that will be used for calibration occurred since the Fragoso Chanell works were taking place.

In this way, it was necessary to change the MDT through the section data obtained through the executive project of the Fragoso channel to make the conditions as close as possible to the reality of the analyzed event. Figure 02 shows the work in progress through the orthophotos in February and the progress until May in the year 2016.

The definition of the geometric characteristics of the HEC-RAS 2D for the construction of the computational flow mesh was carried out considering square cells with 10 m sides for the generation of maps of the extent of the flood and depths of the flood peaks. Square meshes with 2 m and 5 m were tested for more precision for the model, but stability was not obtained. The size and location of the 2D Flow cells are user-defined, and therefore the process requires a priori knowledge of morphology and flow paths in the floodplain. This knowledge of the study area is essential because the HEC-RAS defines the results of a single elevation of water surface for each cell and each face of the cell. The cell's hydraulic gradient is calculated in two dimensions using the complete Saint Venant equations, diffusion wave equations, and mass conservation equations.

For the channeled and natural Fragoso River region, the region of most significant interest, a mesh refinement was carried out through break lines (Break-Lines) and then a reduction in the size of the cells to orient the flow and increase the precision of the model. The dimensions of the cells in the refined areas varied between 2m x 2m until reaching the dimensions of the original mesh of 10m x 10m. Figure 03 shows the two-dimensional mesh generated over the MDT for the channeled and natural Fragoso rivers.

The spatialized Manning roughness coefficient was determined for the entire basin, using the land use and occupation map for 2016 as a reference. The spatialization was divided into six classes: urban area, pasture, agriculture, forest, channeled river, and natural river. The internal boundary conditions for each sub-basin (1 to 8) were determined, inserting the respective input hydrographs for the simulated hydrological event, with a time interval every minute. The tidal curve at the basin outlet was defined as an outlet boundary condition.

The time step used for the simulations was 1 minute, and the intervals of results met the Courant conditions. The post-processing of the two-dimensional simulations was performed in the RasMapper application, using the event of May 30, 2016 (calibration), July 24, 2019 (validation), and the return times of 2, 10, 25, 50, and 100 years.

The depth hazard indicator was used, generating hazard indicator maps for the return time of 2 and 100 years. According to Wright (2008), floods with a water depth of more than 0.60 meters result in a definite danger to people, thus being used to define three levels of severity of the flood for the Fragoso river basin, being classified as the water depth in low (0-0.60 m), medium (0.60-1.2 m) and high (> 1.2 m). The

mapping of hazard indicators helped identify the areas with the most significant potential damage to the population in the Fragoso river floodplain.

For comparison purposes, the map of the hazard indicator about depth for the municipality of Ipojuca in Pernambuco (Ribeiro Neto, 2016), the mapping of the flood hazard areas in the Braço does Baú basin, located in the municipality of Ilhota, Santa Catarina, Brazil (Monteiro and Kobiyama 2013) and risk indices in Dhaka, capital of Bangladesh (Masood and Takeuchi 2012 and Gain et al. 2015).

Brussee et al. (2021) evaluated areas with low altitudes and large potential flood depths and observed that water depth is an essential parameter in the loss of life model and places with many inhabitants, resulting in more considerable loss of life estimates. The results of this study can be used to inform flood modelers, spatial planners, and emergency managers and support decision-makers for flood risk management strategies.

As for categorization, the classification developed by Zonensein (2007) was chosen, which presents the normalization of depths in five empirically defined ranges presented in Table 03 and illustrated in Figure 04.

Table 03 – Normalization ranges of the flood quota. Source: Zonensein (2007)

Height (cm)	Effect
<10	The curb is usually approximately 15 cm high, so at 10 cm, the water is limited to the streets.
50	With 50 cm, the flood floods streets and parks, sidewalks, flowerbeds, backyards, and parking lots. It can interrupt vehicular traffic, especially people, and invade simpler houses, with thresholds close to the sidewalk level.
70	At 70 cm, water has probably already invaded the interior of houses, causing damage to their structure and contents.
100	At this point, the water reaches practically all the goods inside the houses.
> 150	This depth reaches not only goods but is also enough to cause drowning.

2.4 Model Calibration and Validation

The calibration of the hydrodynamic model was carried out by determining the most suitable and stable Manning value for the simulation of the extreme precipitation event that occurred on May 30, 2016.

With the absence of fluviometric stations, the heights of the flood spots were analyzed in a simplified way and confronted with the data measured by a team of topographers after the mentioned event, who carried out the mapping and survey of the geographic coordinates of 20 limiting points of the water in a critical region of the study area, as can be seen in Figure 05, by the initiative of the management team of the

Fragoso Chanell work in partnership with the Federal University of Pernambuco. This survey served as a reference to obtain the maximum levels reached by the flood.

The roughness values were manually modified repeatedly until the observed and simulated points were adequately close in stable simulations.

For statistical evaluation of the performance of the model, observed and simulated data were compared based on several methods such as the Nash and Sutcliffe Efficiency Coefficient (NSE), Coefficient of Determination (R^2), Percent Bias (PBias), and RSR. Zappa (2002) proposes values above 0.5 for NSE. Gotschalk and Motovilov (2000) apud Van Liew et al. (2007) classify NSE values above 0.75 as excellent and acceptable values between 0.75 and 0.36, whether for daily or monthly time steps. Moriasi et al. (2007) classify the R^2 performance indicators with values above 0.5 as satisfactory. The other NSE, Pbias, and RSR for calibration and validation have their performance values indicated in Table 04 below.

Table 04 - Recommended performance values for monthly simulations. Source: Adapted from Moriasi et al. 2007; Ayele et al. 2017

Recommended performance values for monthly simulations	NSE	PBIAS (%)	RSR	R²
Excellent	0,75 a 1,00	< ± 10	0 a 0,5	0,7 a 1,0
Well	0,65 a 0,75	De ± 10 a ± 15	0,5 a 0,6	0,6 a 0,7
Satisfactory	0,50 a 0,65	De ± 15 a 25	0,6 a 0,7	0,5 a 0,6
Unsatisfactory	< 0,50	> ± 25	> 0,7	< 0,5

As input data, hydrographs generated by PCSWMM in the sub-basins were used, with maximum flows shown in Table 05 below. The exit at the meeting with the Paratibe River was considered to exit the system.

Table 05 – Maximum flows per sub-basin for the event on May 30, 2016, in the Fragoso River basin – Olinda/PE. Source: Prepared by the author.

Sub-basin	1	2	3	4	5	6	7	8
Maximum flow (m³/s)	12,59	17,41	56,31	24,30	62,77	54,78	35,41	33,19

The calibrated Manning roughness coefficients were spatialized to consider the scenario closest to reality, with results shown in Table 06 and Figure 06 below.

Table 06 – Calibrated Manning roughness coefficients. Source: Prepared by the author.

Class of use and occupation	Calibrated Manning (n) roughness coefficient
Urban area	0,01
Pasture	0,03
Agriculture	0,04
Forest	0,8
Channeled River	0,016
Natural River	0,035

After the calibration with the event of May 30, 2016, the qualitative validation of the model was carried out with the intense precipitation that occurred on July 24, 2019, to make the predictions later.

An on-site visit was carried out to identify some flooding points and then verified in the model and a survey from some reports, identifying some points such as Caetano Ribeiro Street, Residential Complex Jardim Olinda, and stretches of the PE-15 road. In general, the most affected neighborhoods were Jardim Atlântico, Jardim Fragoso and Casa Caiada. Aerial drone images, provided by a photography and filming company, were also used to map the floods of the study, performing the comparison with the model.

Results And Discussion

The region of the lower city of Olinda, where the Fragoso river is located, has been suffering from flooding during rainy periods for several years. As another example, we have May 9, 2016, when an intense precipitation event was recorded, with an accumulated rainfall of 239 mm in 22 hours. Furthermore, events like February 6, 2019, June 13, 2019, May 23, 2020, and June 14, 2016, have caused the Fragoso channel many flooding and overflow issues.

The problem is mainly caused by the disorderly urban occupation that produces situations of vulnerability:

- - Many houses were built in shallow elevation areas that are frequently flooded;
- - Urbanization invaded the larger bed of the Fragoso River (floodplain). It resulted in the strangulation of the expanded channel of the river, culminating in a decrease in its flow capacity in the wettest winters.
- - The stretch of Alto Fragoso, west of highway PE15, is also being urbanized. Even though urbanization is slower in this stretch, the flows produced in the heavy rains in this part of the basin are already much higher.

Currently, the municipality is undergoing an expansion of its road system to improve traffic conditions in search of better mobility on North Metropolitan Avenue, which integrates PE-15 road (Olinda city) and PE-

01 road (Paulista city). The project, promoted in partnership with the State and Federal Governments, also provides for the channeling of part of the Fragoso River.

The works on the Fragoso chanell were tendered in 2012 and began in September 2013, under the responsibility of Companhia Pernambucana de Habitação e Obras (CEHAB), Secretary of Cities and Olinda City Hall. Currently, the chanell works are managed by CEHAB. However, the Court of Auditors of the State of Pernambuco (TCE-PE) has been working on the project since January 2014 to monitor the contract providing for the coating of the Fragoso Chanell – 2nd Stage the Construction of eight Works of Art.

Given this context, a hydrodynamic simulation was carried out for the future scenario with the chanell work completed, mapping the floodable areas for return times of 2 and 100 years. A constant rectangular section of 45 meters wide was considered. The model was also adapted about the Manning coefficient to modify the spatialization of the natural river to the channeled river.

Hydrological modeling in the Fragoso River Basin was carried out in 8 sub-basins, as shown in Fig. 07 below. The input parameters in the PCSWMM model, obtained for each sub-basin, are shown in Table 07.

To determine the impermeabilization rate, georeferenced images from the Landsat 8 OLI-TIRS satellite of 08/27/2018, orbit/point 214/065, made available by the United States Geological Survey (USGS), were used. First, an unsupervised soil classification was carried out, focusing on identifying permeable and impermeable areas for each study sub-basin. The dated image was chosen due to the lower presence of clouds. The result of the impermeabilization ratio is a mesh with two colors, one for the impermeable area and one for the permeable area. After the classification was performed, comparisons were made with current Google Earth images, confirming good accuracy. A densely urbanized area with few permeable areas was observed during the registration of areas since the occupation process is heavily urbanized. As well as another area with a significant presence of permeable areas and a strong tendency of areas to be occupied.

Table 07
– Input data of the PCSWMM model sub-basins.

Source: Prepared by the author.

Sub-basin	Area (ha)	Surface width (m)	Slope (m/m)	Impermeable area
01	326,440	587,92	0,0049	16,24%
02	274,680	489,63	0,0058	35,49%
03	548,120	619,06	0,0025	42,60%
04	231,080	560,86	0,0047	21,70%
05	679,400	622,08	0,0030	43,00%
06	342,640	750,78	0,0004	74,46%
07	225,200	353,23	0,0003	84,86%
08	230,120	416,56	0,0012	84,56%

Some parameters, such as the storage in depressions, which is the maximum storable value at the surface by flooding, waterlogging, and an interception for impermeable and permeable areas, were determined according to the PCSWMM user manual. In addition, the Manning coefficient "n" for surface runoff in the impermeable and permeable sub-basin and the values for the conduits were also determined using the manual (Rossman 2016). The values can be seen in Table 08.

Table 08
– Parameters determined for input data in the PCSWMM model.

Source: Prepared by the author.

Storage in depressions (mm)		Manning roughness coefficient			
Permeable	Impermeable	Permeable	Impermeable	Coated channels	Natural channels
5,08	2,54	0,15	0,024	0,013	0,040

Regarding infiltration, the Curve Number model was used. The CN's obtained for each sub-basin are presented in Table 09. The drying time, which is the number of days it takes a fully saturated soil to dry, of 7 days, was considered a standard average reference for this study. However, typical values can vary between 2 and 14 days.

Table 09
– Curve-Number Coefficient (CN) for each sub-basin.

Source: Prepared by the author.

Sub-basin	1	2	3	4	5	6	7	8
CN	51	65	61	61	70	79	94	94

Regarding the rainfall data, the extreme rainfall event of May 30, 2016, was used, which caused numerous problems for the Metropolitan Region of Recife population. Data from Cemaden were used, where it can be seen that the event caused an accumulated rain of 241 mm distributed in 16 hours, as shown in Fig. 08. The most intense period of precipitation was concentrated in 3 hours, starting at 07:00 hours, resulting in total precipitation of 168 mm in the Jardim Fragoso pluviometric station. The tide was relatively high in this most critical interval, at 1.69 meters.

The tide is an essential data that needs to be evaluated together with the rainfall data in the hydrological and hydrodynamic model, as it influences the flooding behavior. The tidal curve that occurred on the day of the analyzed event is shown in Fig. 09 below.

The PCSWMM software presented as continuity errors the values presented in Table 10 for the calibration simulation and the different simulated return times lasting 180 minutes (estimated concentration-time for the Fragoso river basin by the Kirpich method). All the errors obtained were below the maximum tolerable of 10%, indicating satisfactory results and good quality simulations.

Table 10
– Continuity errors for simulations without control alternatives.

Source: Prepared by the author.

Return time	Continuity errors (%)	
	Surface runoff	Flow propagation
Calibration	-0,03%	-0,48%
2 years	-0,05%	-0,41%
10 years	-0,06%	-0,32%
25 years	-0,06%	-0,28%
50 years	-0,06%	-0,24%
100 years	-0,07%	-0,46%

Figure 10 shows the flooded patch estimated by the two-dimensional hydrodynamic simulation for the intense precipitation event on May 30, 2016, with the physical characteristics in the digital terrain model for 2016. The analysis showed a flooded area of 2.86 km². According to this simulation, the neighborhoods Jardim Atlântico, Fragoso, Jardim Fragoso, and the western part of Casa Caiada were the most affected.

The maximum flood depths (simulated and observed) were then compared. As can be seen, by Batista (2020), the degree of accuracy of the results of a model is associated with different factors, in a particular way and together. Furthermore, the uncertainties involved in the various modeling stages limit the accuracy of the results, as in the case of several hydrological model parameters whose values are

estimated through physical properties. The values of the statistical coefficients obtained for the calibration of the Fragoso River basin are shown in Table 11 below.

Table 11
– Statistical calibration coefficients for the Fragoso River basin.

Source: Prepared by the author.

Statistical Coefficients	Values obtained with the calibration for 05/30/2016
NSE	0.685
R^2	0.777
PBIAS	6.110
RSR	0.562

The NSE statistical coefficient showed good performance, being situated between the limits of 0.65 to 0.75; R^2 presented an excellent performance for being framed between the limits 0.7 to 1.0. For the statistical coefficient PBIAS, the performance was excellent since the value obtained by the analysis of the simulations is less than 10. Finally, the RSR presented good performance, framed between the thresholds of 0.5 to 0.6. In general, it is observed that the statistical results were presented satisfactorily by the values recommended by the literature and described above.

Batista (2020) used the statistical coefficients R^2, NSE, and PBIAS to evaluate the modeling performance for the Pirapama river basin in the municipality of Cabo de Santo Agostinho in Pernambuco. Shawul et al. (2019) also used the R^2, NSE, PBIAS, and RSR indicators to evaluate their simulations in the Upper Awash basin in Ethiopia.

In this way, the model presented itself satisfactorily and coherently with reality and is then used for the scenarios presented below. For example, Fig. 11 would show the flooding patch with a simulation of the precipitation event on May 30 if the Fragoso chanell work had already been completed. With Fig. 12 and Fig. 13, it is possible to observe the flood maps referring to the simulations carried out with the calibrated roughness coefficients for the return time of 2 and 100 years, respectively.

In terms of a comparative analysis of the total flooded area and the maximum height reached in the main channel of the Fragoso River, the results presented in Table 12 below were obtained.

Table 12
– Comparison between flooded areas and maximum heights reached, considering the Fragoso chanell work completed.

	Return time (Tr)				
	2 years	10 years	25 years	50 years	100 years
Maximum flooded area	1,65 km²	1,73km²	1,87km²	1,93km²	2,00km²
The maximum height reached in the main channel (inside the Fragoso river)	4,40m	4,60m	4,76m	4,90m	5,05m

This study clearly shows that the flooding problems will persist even after completing the chanell works. The simulations were carried out to consider the free flow of water in the channel. However, in real situations, problems such as silting and garbage are present in the channel, which can distort the results, increasing the areas of flooding and the heights reached.

The mapping of hazard indicators helped identify the areas with the most significant potential damage to the population in the Fragoso River floodplain, serving as a reference for flood risk management, including spatial planning and prioritization of necessary measures. The water depth was an essential factor in analyzing post-flood scenarios to characterize the level of danger. This indicator is a good choice due to the predominantly residential land use.

The mapping of areas in the analyzed region shows the positive potential of the method to identify places that may suffer damages caused by floods. Figures 14 and 15 illustrate the limits of the Fragoso river flooded area for a return period of 2 and 100 years, respectively, obtained from the HEC-RAS model.

In the past, the floodplains were the natural control of water, as the riverside soil was naturally prepared to be flooded in times of flood, absorbing much of the water that overflowed and using its nutrients. Today, riverine floods advance along the larger bed of streams and rivers, usually delimited by floods of around 100 years of recurrence, with urban occupation already established, whether for housing, recreation, agricultural, commercial or industrial use, its roads and buildings become doomed to potential damage. This justifies the importance of prior delimitation of floodable areas adjacent to streams as a helpful instrument in urban planning (Oliveira 2016 and Filho 2017).

In this way, measures for the zoning of floodable areas are essential for planning municipalities that develop along the rivers, as they mitigate the recurring damages of floods. In addition, flood maps support the reorganization of urban space, as they can help establish new occupation guidelines in a city (Oliveira 2017).

Long-term mitigation measures and strategies need to be implemented with the public to avoid severe damage from heavy rains. Predicting early warnings and subsequent actions requires reliable knowledge of hazard prediction at appropriate spatial and temporal scales and sufficient lead times; the time

between threat notification and a flood event is considered the minimum time required to implement practical actions (Young et al. 2021).

Conclusions

The present study allowed us to evaluate some flooding situations in the Fragoso river basin in the city of Olinda in response to different rainfall events of medium and high intensity in the northern part of the Recife Metropolitan Region in Pernambuco State, Brazil.

Geographic and social peculiarities influence Fragoso river floods. Leading causes are a rapid increase in demographic density, advances in urbanization, a high rate of soil impermeabilization, sizeable flat plain, and low terrain height above sea level.

A hydrological condition that influences floods are excessive rainfall (sometimes more than 200mm a day), low hydraulic gradient, high water table, and high tides. If heavy rains are simultaneous to high tide, all the regions of the Fragoso river basin will be flooded.

To carry out the simulations, the SWMM hydrological model and the HEC-RAS hydrodynamic model were used, which presented good performance for the analyzes carried out, showing consistency with the floods that occur in the region. Furthermore, the continuity errors obtained in all stages were consistently below 10%, indicating a good quality of the results obtained. For the two-dimensional modeling, the resolution of the MDT in the scale of 1:1000 provided by the PE3D proved to be fundamental for a better representation of the results.

With the Fragoso chanell work carried out, the maximum flooded areas vary from 1.65 km² to 2.00 km² for the return period of 2 and 100 years, respectively. In this way, it can be seen that there is a reduction in flooding after the completion of the channel, but that the flooding problems will persist.

Risk analysis is essential for planning and intervention in flood-prone areas. Hazard maps for a return period of 2 and 100 years help identify areas with the most significant potential harm to the population. In addition, the spatial details of hazard indicators are valuable for flood risk management, as the map provides a more direct and faster assessment than other methods.

The Fragoso River basin has problems of flooding, which are accentuated mainly by the disorderly occupation. Many residences were built in very low-level places, which are often flooded. Other houses irregularly occupied the floodway banks of Fragoso River, with the strangulation of the river channel and consequently the decrease in the flow capacity.

For the construction of Perimetral Avenue, measures were adopted to relocate the residents to a more suitable region, improving the river's outflow capacity. However, houses not so close to the river but at shallow levels will continue to suffer flooding.

An essential point in the analysis of floods in the Fragoso basin is the downstream boundary condition at the mouth of the Fragoso River in the final stretch of the Paratibe River (a neighbor basin with a shared mouth to the sea), close to the Janga bridge. If the water level of the Paratibe River is too high, it makes it difficult for the waters of the Fragoso River to flow into the mouth, damming the waters and worsening the floods. The causes for the high level of Paratibe can be hefty rains in the Paratibe basin in the municipality of Paulista, high syzygy tides, and the rise in sea level due to climate change.

Declarations

Acknowledgements The author would like to thank the Foundation for the Support of Science and Technology of Pernambuco (FACEPE).

Authors contribution ABR contributed to conceptualization, methodology, software, writing—original draft, data curation. JJSPC contributed to supervision, project administration, writing—review and editing, conceptualization.

Conflict of interest The authors declare that they have no known competing financial interests or personal relationships that could have appeared to influence the work reported in this paper.

References

Adams, S.; Aich, V.; Albrecht, T.; Baarsch, F.; Boit, A.; Canales Trujillo, N.; Cartsburg, M.; Coumou, D.; Eden, A.; Fader, M.; Hare, B.; Hoff, H.; Jobbins, G.; Jones, L.; Kit, O.; Krummenauer, L.; Langerwisch, F.; Le Masson, V.; Ludi, E.; Marcus, R.; Mengel, M.; Mosello, B.; Möhring, J.; Norton, A.; Otto, I. M.; Perette, M.; Pereznieto, P.; Rammig, A.; Reckien, D.; Reinhardt, J.; Reyer, C.; Robinson, A.; Rocha, M.; Sakschewski, B.; Schaeffer, M.; Schaphoff, S.; Schewe, J.; Schleussner, C.; Serdeczny, O.; Stagl, J.; Thonicke, K.; Waha, K. & World, B. Latin America and the Caribbean: 4o Turn down the heat - confronting the new climate normal. World Bank Group. V2. 2014. 275p.

Batista, L. F. D. R.; Ribeiro Neto, A.; Coutinho, Q. Flood Damage Analysis: A Brazilian Case Study. Journal of Urban and Environmental Engineering, v.14, nº 1, p.150-160, 2020. https://doi.org/10.4090/juee.2020.v14n1.150160

Brussee Ar, Bricker Jd, De Bruijn Km, Verhoeven Gf, Winsemius Hc, Jonkman Sn. Impact of hydraulic model resolution and loss of life model modification on flood fatality risk estimation: Case study of the Bommelerwaard, The Netherlands. J Flood Risk Management. 2021; 14:e12713. https://doi.org/10.1111/jfr3.1271

Cirilo, J. A.; Alves, F. H. B.; Silva, L. A. C.; Campos, J. H. De A. L. Suporte de Informações Georreferenciadas de Alta Resolução para Implantação de Infraestrutura e Planejamento

Territorial. 2014. Revista Brasileira de Geografia Física, vol 07, n.04 (2014) 755-763

Elkhrachy I, Pham Qb, Costache R, Et Al. Sentinel-1 remote sensing data and Hydrologic Engineering Centres River Analysis System two-dimensional integration for flash flood detection and modeling in New Cairo City, Egypt. J Flood Risk Management. 2021;14: e12692. https://doi.org/10.1111/jfr3.12692

Filho, J.E.A.; Salla, M.R.; Reis, A.; Jhunior, H.C. Da S. Influência da progressiva ocupação urbana na ocorrência de áreas inundáveis. 2017. Ciência & Engenharia. v. 26, n. 2, p. 21 – 31, jul. – dez. 2017

Frank, B.; Pinheiro, A. Enchentes na bacia do Itajaí: 20 anos de experiências. 1. ed. Blumenau: Editora da FURB, 2003. 237 p.

Gain, A.K.; Mojtahed, V.; Biscaro, C.; Balbi, S.; Giupponi, C. An integrated approach of flood risk assessment in the eastern part of Dhaka City. Natural Hazards, v. 79, n. 3, p. 1499-1530, 2015.

Hodgkins, G.; Dudley, R.; Archfield, S.; Renard, B. Effects of climate, regulation, and urbanization on historical flood trends in the United States. Journal of Hydrology, v. 573, p.697-709, Jun. 2019.

Instituto Hidrográfico. Tabela de Marés – Generalidades, I, 199 págs., Lisboa, Portugal, 2018.

IPCC, 2021: Climate Change 2021: The Physical Science Basis. Contribution of Working Group I to the Sixth Assessment Report of the Intergovernmental Panel on Climate Change [Masson-Delmotte, V., P. Zhai, A. Pirani, S.L. Connors, C. Péan, S. Berger, N. Caud, Y. Chen, L. Goldfarb, M.I. Gomis, M. Huang, K. Leitzell, E. Lonnoy, J.B.R. Matthews, T.K. Maycock, T. Waterfield, O. Yelekçi, R. Yu, and B. Zhou (eds.)]. Cambridge University Press. In Press.

Itagaki O, Bermudez Dbs, Zemmoto T, Ohara M. Proposal of a method for assessing combined flood risk reduction effect by hazard control measures and exposure reduction measures based on limited data. J Flood Risk Management. 2021;14:e12714. https://doi.org/10.1111/jfr3.12714

Kulp, Scott A.; Strauss, Benjamin H. New elevation data triple estimates of global vulnerability to sea-level rise and coastal flooding. Nature Communications. 2019, 10:4844. https://doi.org/10.1038/s41467-019-12808-z

Masood, M.; Takeuchi, K. Assessment of flood hazard, vulnerability, and risk of mid-eastern Dhaka using DEM and 1-D hydrodynamic model. Natural Hazards, v. 61, n. 2, 757-770, 2012

Momo, M. R.; Pinheiro, A.; Severo, D.L.; Cuartas, L.A.; Nobre, A.D. Desempenho do modelo HAND no mapeamento de áreas suscetíveis à inundação usando dados de alta resolução espacial. Revista Brasileira de Recursos Hídricos. Versão On-line ISSN 2318-0331. RBRH vol. 21 nº.1 Porto Alegre jan./mar. 2016 p. 200 – 208

Monteiro, L. R.; Kobiyama, M. Proposta de metodologia de mapeamento de perigo de inundação. REGA, v. 10, p. 13-25, July/Dec. 2013.

Moriasi, D. N.; Arnold, J. G.; Van Liew, M. W.; Bingner, R. L.; Harnel, R. D.; Veith, T. L. 2007. Model evaluation guidelines for systematic quantification of accuracy in watershed simulations. American Society of Agricultural and Biological Engineers. Vol. 50(3): 885–900

Nogherotto, R., Fantini, A., Raffaele, F., Di Sante, F., Dottori, F., Coppola, E., & Giorgi, F. (2022). A combined hydrological and hydraulic modeling approach for the flood hazard mapping of the Po river basin.Journal of Flood Risk Management,15(1), e12755.https://doi.org/10.1111/jfr3.12755

Oliveira, F.A. De.; Arantes, C.Q.; Oliveira, J.A.De.; Pereira, T.S.R.; Formiga, K.T.M. Determinação do limite da faixa de inundação com uso do HEC-RAS para o parque linear do Córrego Macambira em Goiânia, Goiás. 2016. Revista Eletrônica de Engenharia Civil. Volume 11, nº 1, 57-66.

Recife. Estudo e Concepção do Plano de Manejo de Águas Pluviais do Recife – PDDR-, disponível na EMLURB. Recife, 2016.

Ribeiro Neto, A.; Batista, L. F. D. R.; Coutinho, R. Q. Methodologies for generating hazard indicator maps and flood-prone areas: municipality of Ipojuca/PE. RBRH vol. 21 nº.2 Porto Alegre abr./jun. 2016 p. 377 – 390

Rossman, L. A.; Huber, W. C. Storm Water Management Model Reference Manual Volume I – Hydrology (Revised). Cincinnati: National Risk Management Laboratory Office Of Research And Development U.s. Environmental Protection Agency, 2016. 233 p.

Shawul, A. A.; Chakma, S.; Melesse, A. M. 2019. The response of water balance components to land cover change is based on hydrologic modeling and partial least squares regression (PLSR) analysis in the Upper Awash Basin. Journal of Hydrology: Regional Studies 26 (2019) 100640

Usace. River Analysis System HEC-RAS: Hydraulic Reference Manual. 2016b. Version 5.0. United States Army Corps of Engineers - USACE. Hydrologic Engineering Center – HEC. Davis, California, EUA, 547 p.

Usace. River Analysis System HEC-RAS: User's Manual. 2016a. Version 5.0. United States Army Corps of Engineers - USACE. Hydrologic Engineering Center – HEC. Davis, California, EUA, 962 p.

Van Liew, M. W; Veith, T.L.; Arnold, J.G. Suitability of SWAT for the Conservation Effects Assessment Project: Comparison on USDA Agricultural Research Service Watersheds. Journal Of Hydrologic Engineering, v. 12, n. 2, p.173-189, 2007.

Wright, J. M. Floodplain Management: Principles and Current Practices. Knoxville: The University of Tennessee, 2008.

Young A, Bhattacharya B, Zevenbergen C. A rainfall threshold-based approach to early warnings in urban data-scarce regions: A case study of pluvial flooding in Alexandria, Egypt. J Flood Risk Management. 2021;14:e12702. https://doi.org/10. 1111/jfr3.1270

Zappa, M. Multiple-response verification of a distributed hydrological model at different spatial scales. Zurich: Swiss Federal Institute of Technology, 2002. 167p. P.hD. Thesis.

Zonensein, J. Índice de risco de cheia como ferramenta de gestão de enchentes. 2007. 105 f. Dissertação (Mestrado em Engenharia Civil) - Universidade Federal do Rio de Janeiro, Rio de Janeiro, 2007.

Figures

Figure 1

Location of the Fragoso River Basin in Olinda – PE. Source: Prepared by the author.

Figure 2

Comparison of the images obtained from the orthophotos (left) and Google Earth (right) for analysis of the alteration of the terrain with the progress of the construction of the channel. Source: Prepared by the author.

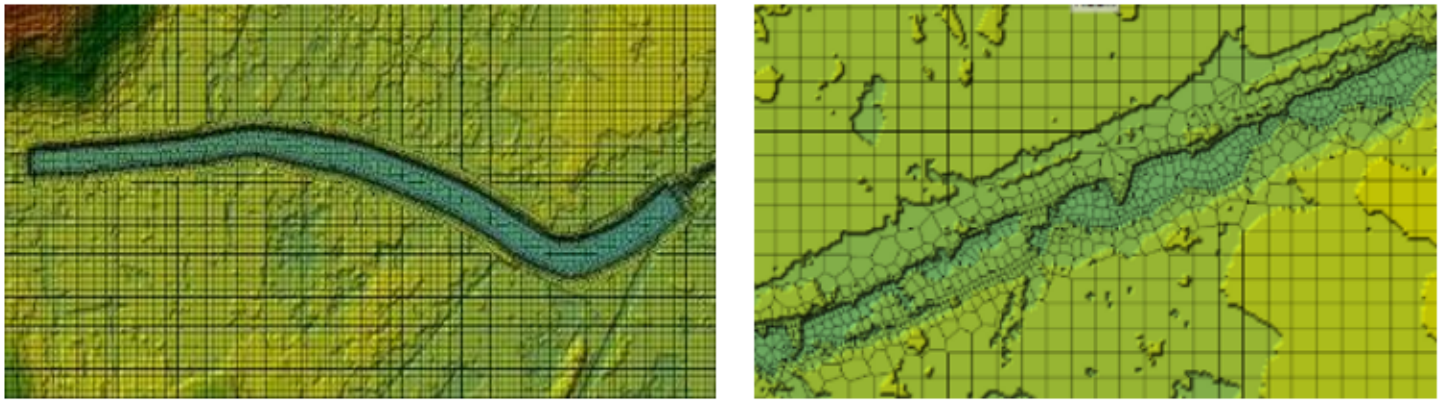

Figure 3

Mesh refinement for the Fragoso river in Olinda-PE. Source: Prepared by the author.

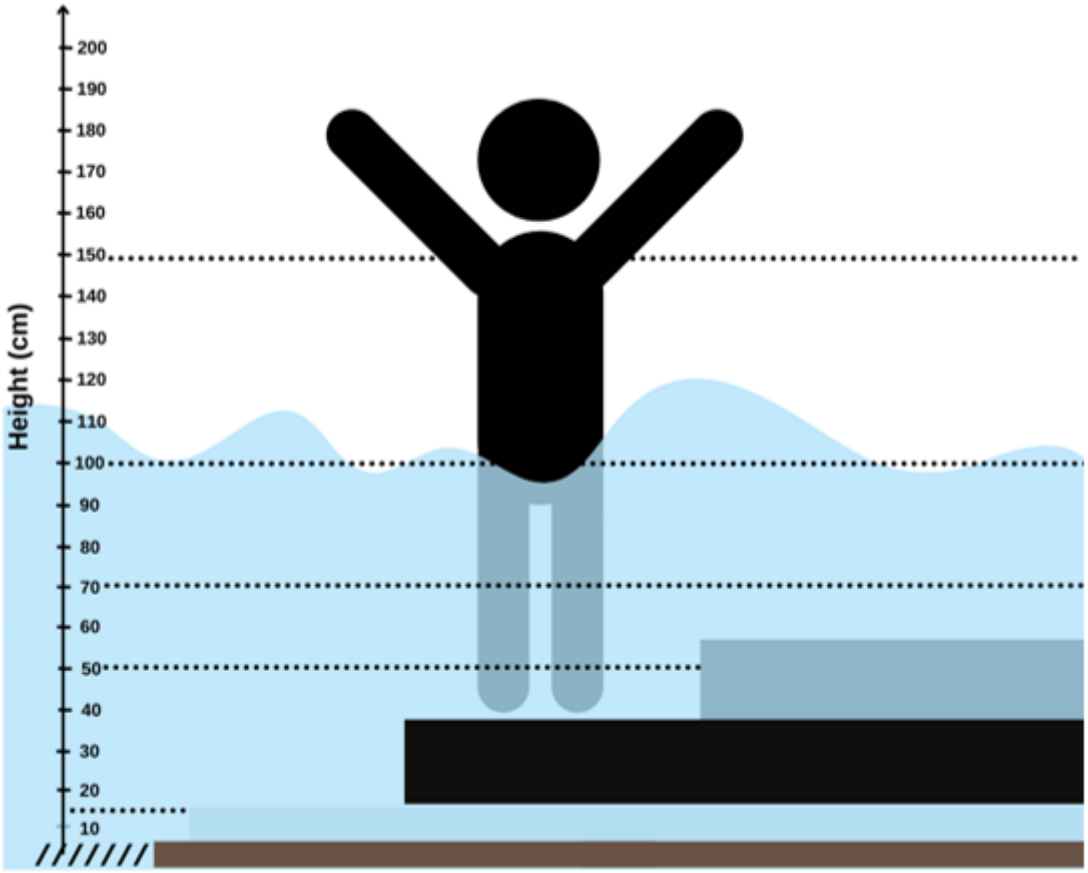

Figure 4

Representation of depth normalization ranges. Source: Adapted from Zonensein (2007)

Figure 5

Distribution of points used for calibration. At each point, maximum flood height has been registered. Source: Prepared by the author.

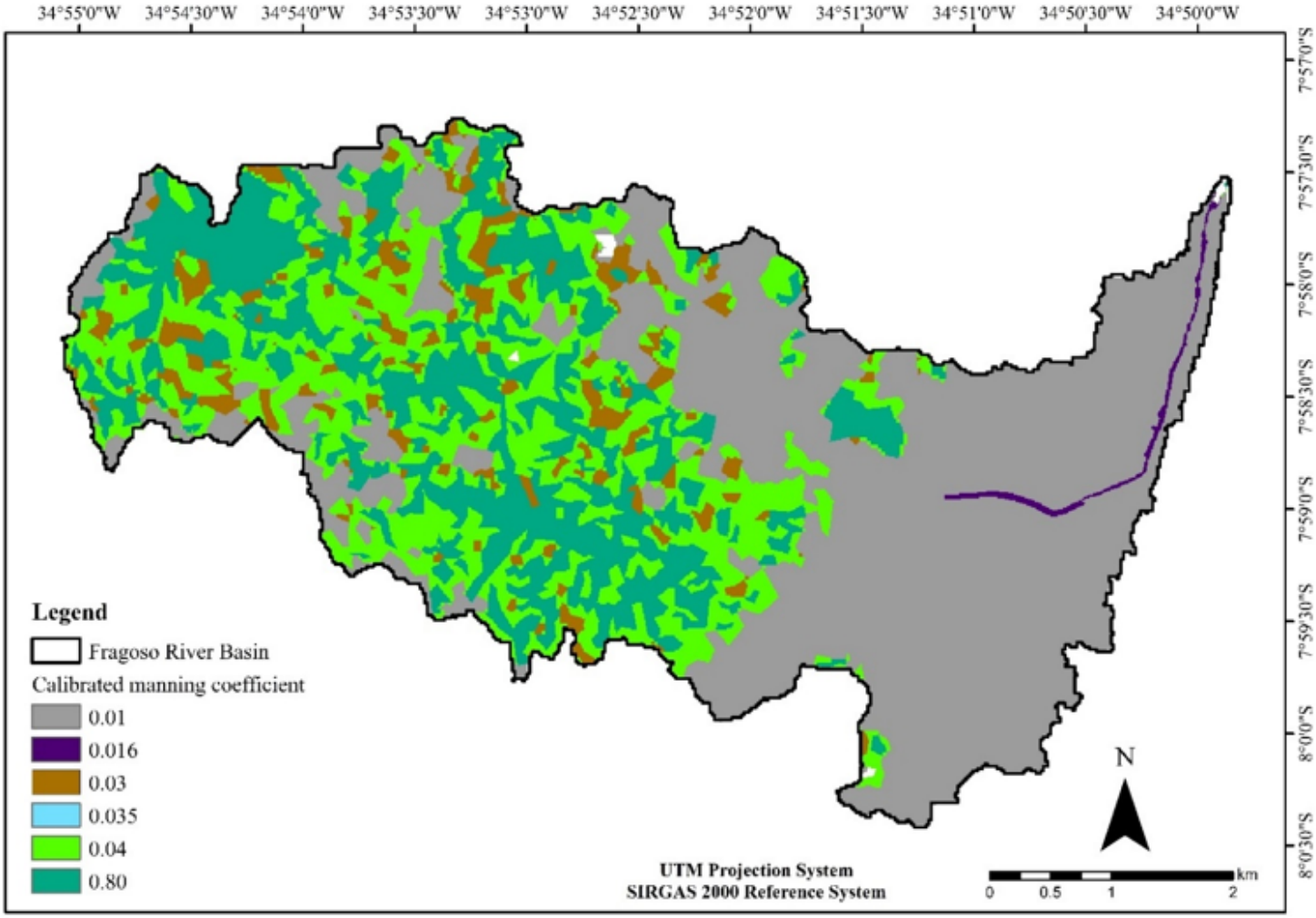

Figure 6

Manning coefficient spatialized for the Fragoso river basin considering the channeled river in the stretch of the plain. Source: Prepared by the author.

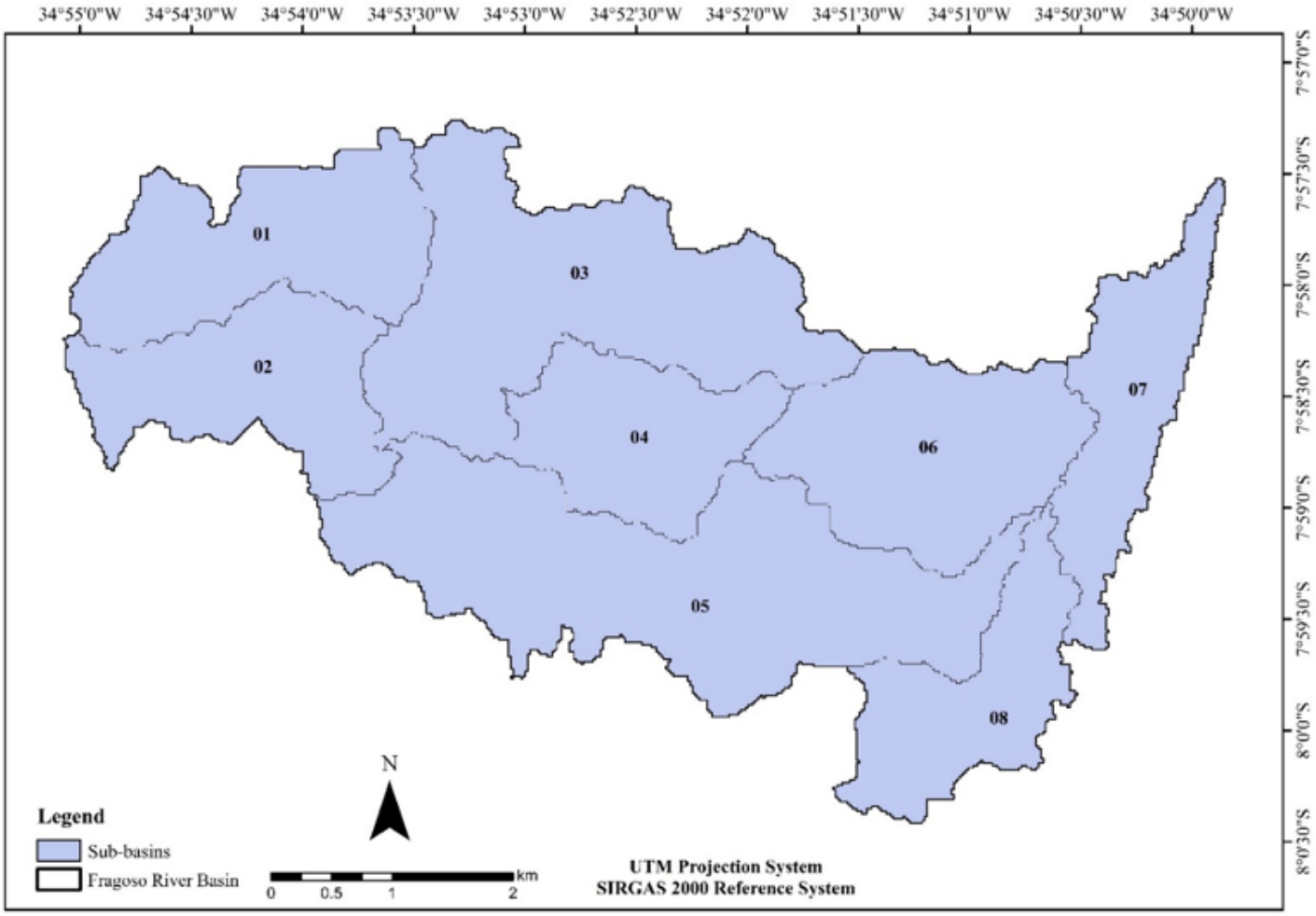

Figure 7

Division of sub-basins in the Fragoso River Basin. Source: Prepared by the author.

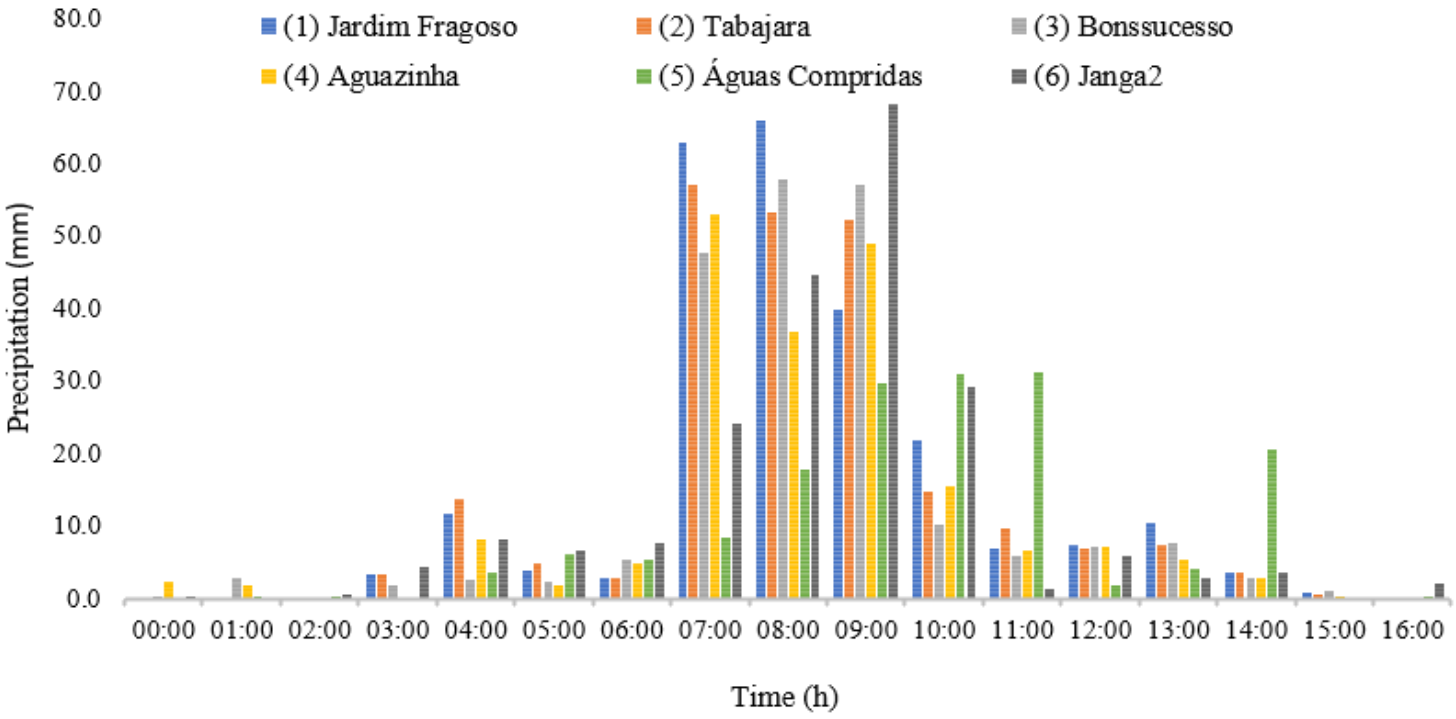

Figure 8

Temporal rainfall variability on May 30, 2016, at the Fragoso River Basin stations. Source: Prepared by the author using data from Cemaden.

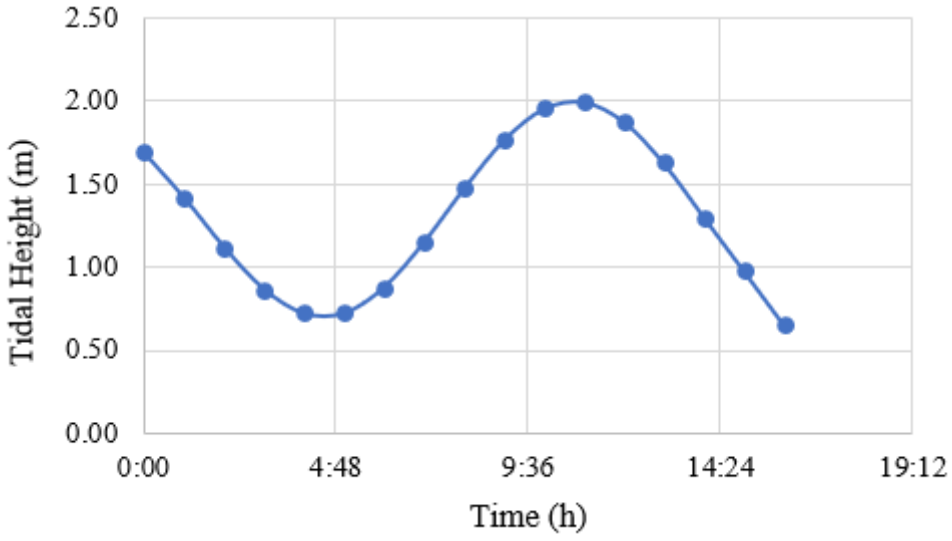

Figure 9

Tide curve for the heavy rainfall event on May 30, 2016. Source: Prepared by the author.

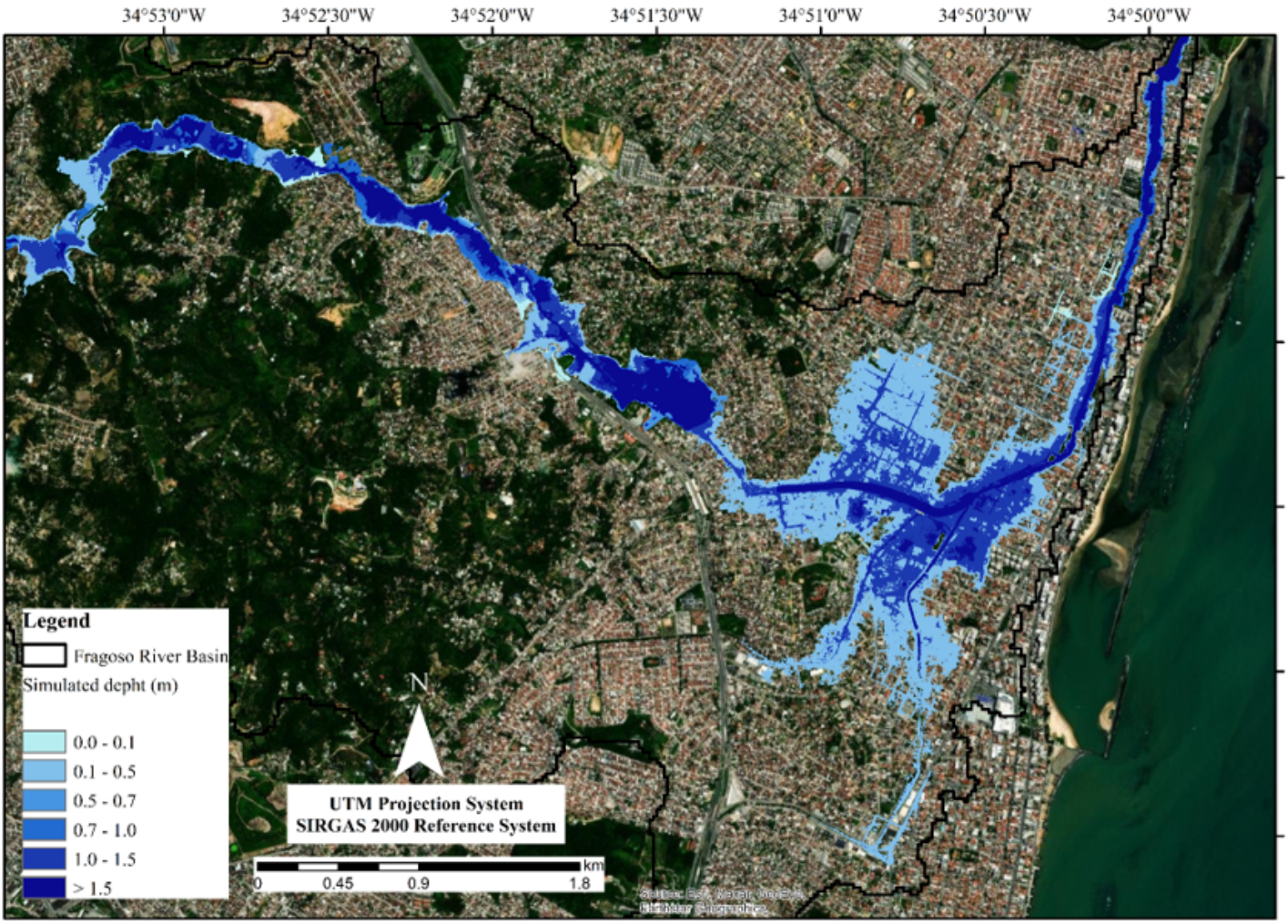

Figure 10

Flood patch map in the Fragoso River Basin for the extreme rainfall event on May 30, 2016. Source: Prepared by the author.

Figure 11

Map of the flooded spot in the Fragoso River Basin for the extreme rainfall event on May 30, 2016, considering the chanell work completed.

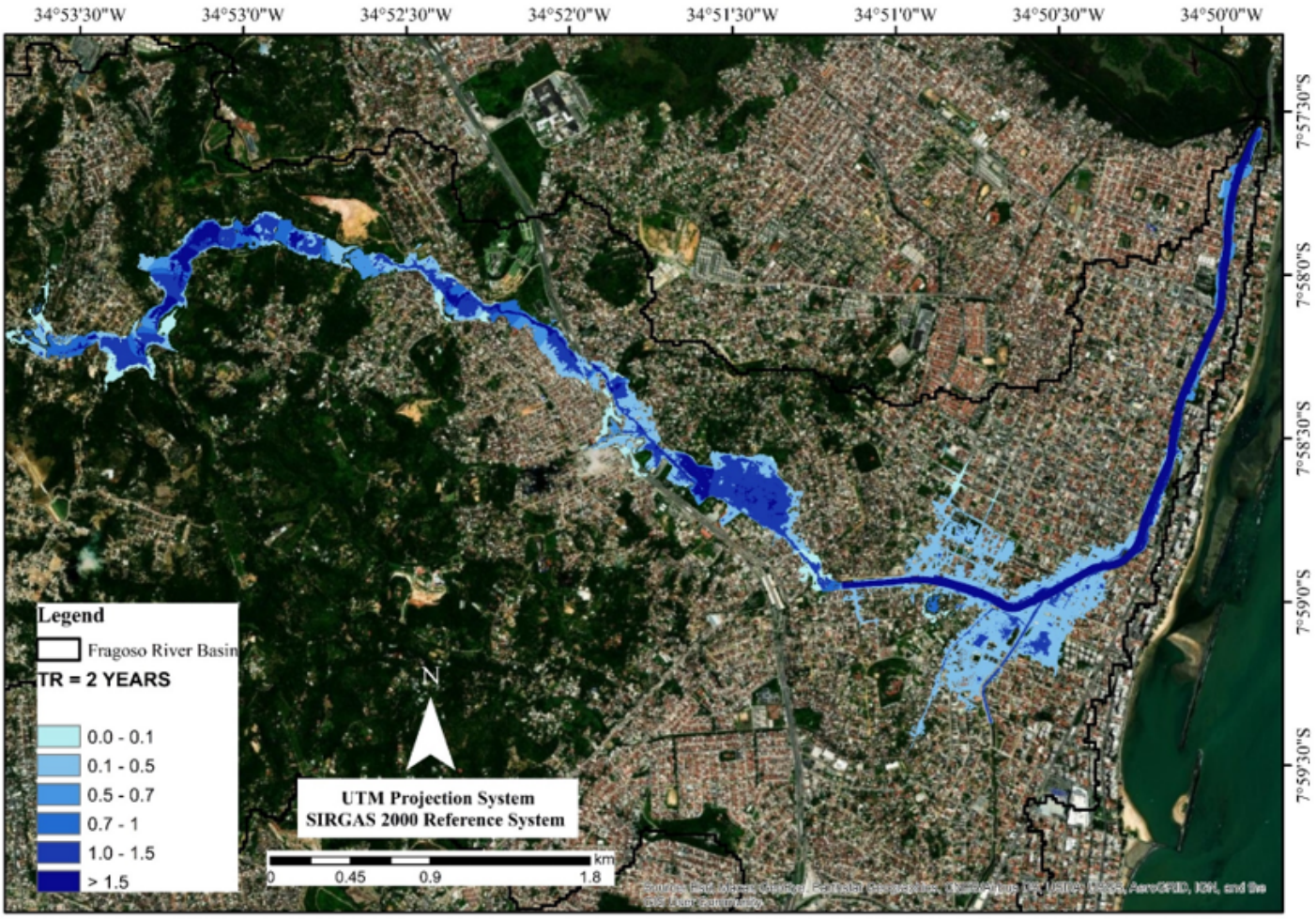

Figure 12

Map of the flooded spot in the Fragoso River Basin for the return time of 2 years considering the chanell work completed.

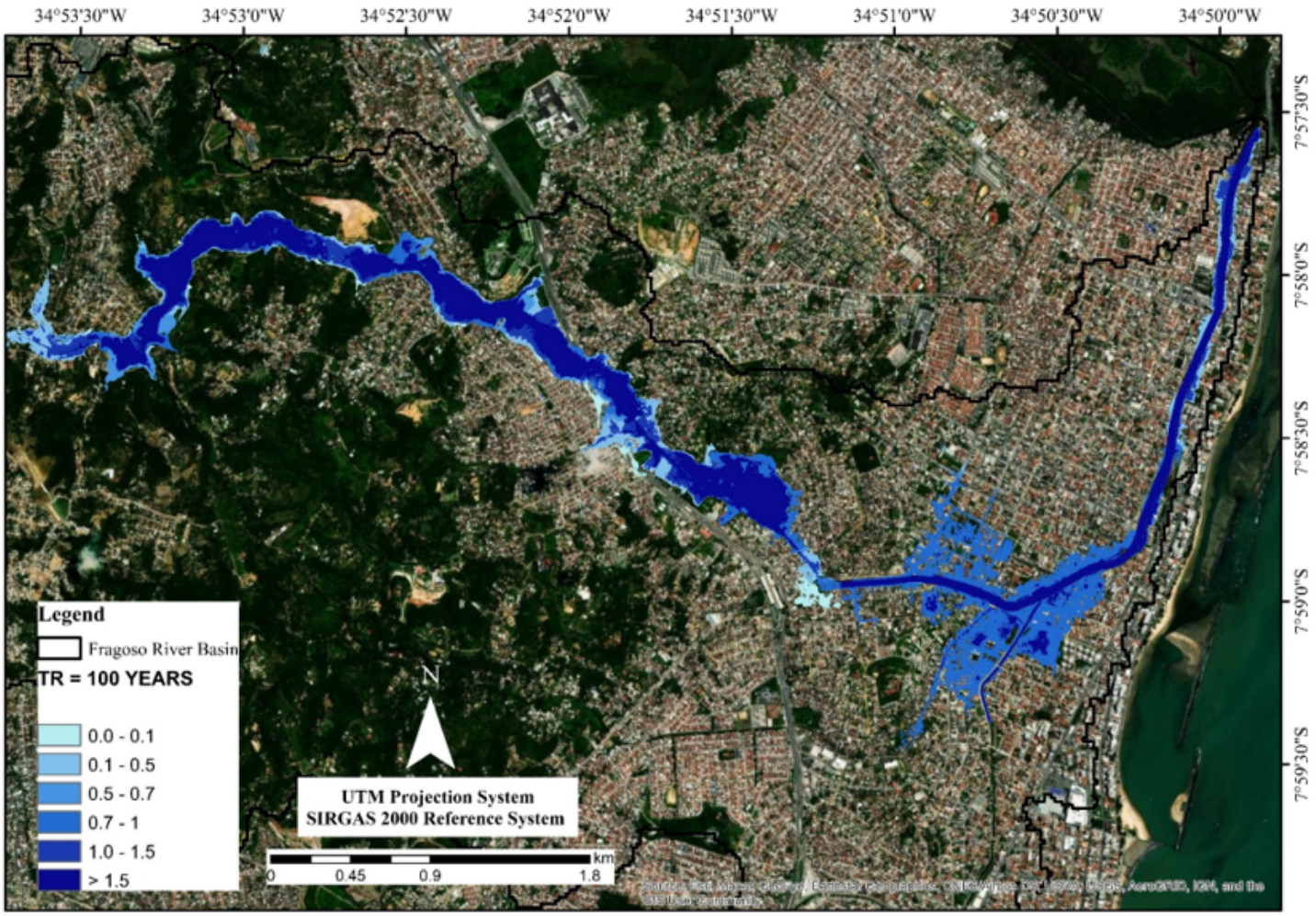

Figure 13

Map of the flooded spot in the Fragoso River Basin for the return time of 100 years considering the chanell work completed.

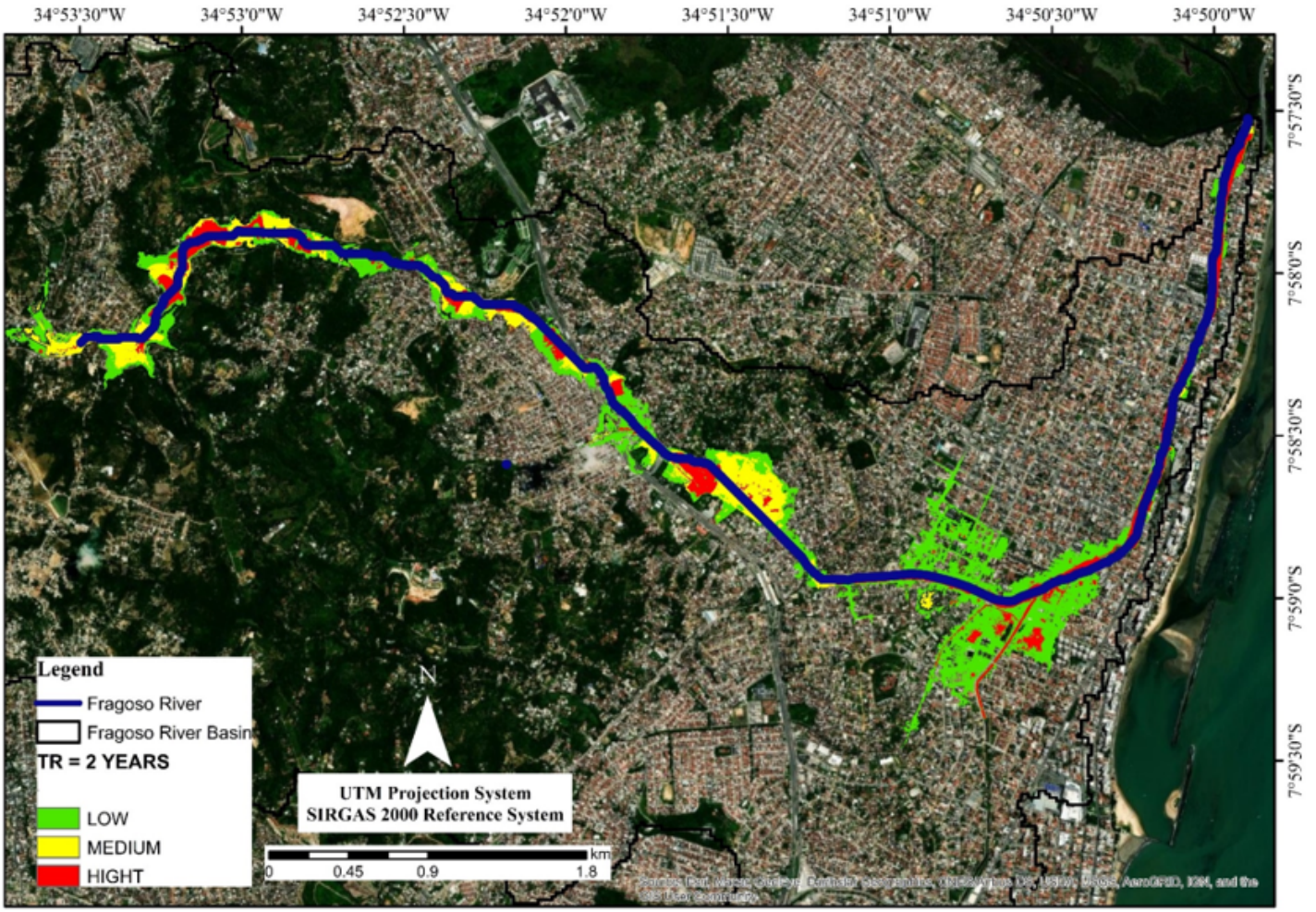

Figure 14

Map of the hazard indicator resulting from flooding for the 2-year return period considering the chanell work completed.

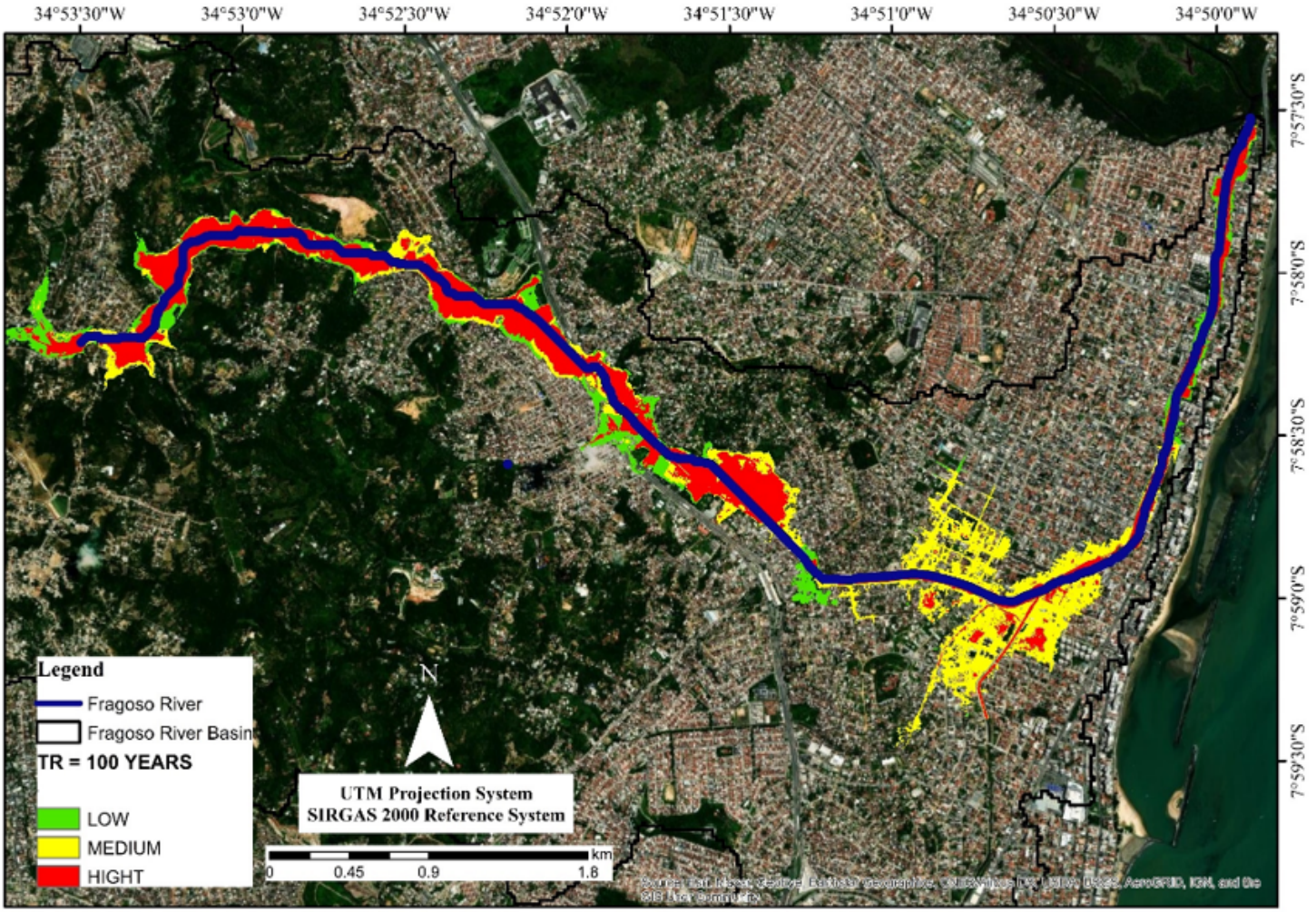

Figure 15

Map of the hazard indicator resulting from flooding for the return period of 100 years considering the chanell work completed.